

Vibrational dynamics in isotopically substituted vitreous GeO₂

F. L. Galeener and A. E. Geissberger
Xerox Palo Alto Research Center, Palo Alto, California 94304

G. W. Ogar, Jr.*
Department of Chemistry, Brown University, Providence, Rhode Island 02912

R. E. Loehman†
S. R. I. International, Menlo Park, California 94025
 (Received 16 May 1983)

We report the polarized Raman spectra of vitreous Ge¹⁶O₂, Ge¹⁸O₂, ⁷⁰GeO₂, and ⁷⁴GeO₂. This yields the ¹⁶O→¹⁸O and ⁷⁰Ge→⁷⁴Ge isotopic shifts for nearly all vibrational modes of the pure glassy material. The shifts of the broad high-frequency (infrared-active) modes are as predicted by a nearest-neighbor central-force ideal continuous-random-network model. The shift of the broad dominant Raman line indicates a small but significant dependence on the Ge mass, and this suggests an effect of disorder not included in the central-force theory. The narrow "defect" line at 530 cm⁻¹ appears to be all oxygen motion, and is tentatively identified with a regular ring of bonds. The narrow line at 345 cm⁻¹ is unique in that it exhibits very little oxygen shift; it seems to consist largely of Ge motion, for which we have no firm explanation.

INTRODUCTION

Measurement of the isotope shifts of the vibrational frequencies of pure glasses have only recently been carried out on a small number of materials¹⁻⁴; they have proven very useful in identifying the origin of spectral features, particularly the relatively narrow lines that have been assigned by Galeener⁵⁻⁷ to regular rings of bonds in the otherwise disordered networks. In particular, Galeener and Mikkelsen¹ have reported ¹⁶O→¹⁸O isotope shifts in vitreous (*v*-) SiO₂, while Galeener and Geissberger² have reported the ²⁸Si→³⁰Si shifts in the same material. The latter authors³ have also reported the ¹⁰B→¹¹B cation isotope shifts in *v*-B₂O₃ and found *no shift* for the sharp 808-cm⁻¹ line that is widely believed to be due to planar B₃O₃ (boroxol) rings.⁸ Similar data on *v*-B₂O₃ have been measured independently by Windisch and Risen,⁴ who also reported ¹⁶O→¹⁸O shifts in *v*-B₂O₃.

In this paper we report careful measurements of the ¹⁶O→¹⁸O and ⁷⁰Ge→⁷⁴Ge isotope shifts in pure *v*-GeO₂. The largest oxygen isotope shifts (45 cm⁻¹) are similar to those seen in *v*-SiO₂ (Ref. 1) and *v*-B₂O₃ (Ref. 4); however, the largest cation shifts (6 cm⁻¹) are at least 3 times smaller than in *v*-SiO₂, and this places serious demands on experimental techniques since some of the lines are ~100 cm⁻¹ wide. We draw our conclusions largely from the oxygen shifts and regard the germanium shifts as merely consistent or supportive.

The structure of *v*-GeO₂ is commonly taken to be a continuous random network (CRN) of GeO₄ tetrahedra which shares corners only, not edges. We find that the isotope shifts of the major (broad) features of the Raman spectra are consistent with this model. However, the isotope shifts of two weak (narrow) Raman lines are not predicted by the CRN model *when evaluated in central forces only*. These two narrow lines may represent defects (point or ring) in the actual glass structure, inadequacies in the

idealized form of the CRN structure used in our analysis, or artifacts due to the absence of noncentral forces in our force-constant model. These possibilities are elaborated upon in the section entitled General Comments.

SAMPLE PREPARATION

The ¹⁸O sample with natural-abundance Ge (atomic wt. of 72.6) was prepared in powdered form via the hydrolysis of GeCl₄ with H₂O enriched⁹ to 98 at. % ¹⁸O. The procedure was developed¹⁰ at the Department of Chemistry, Brown University, and has been used¹¹ for the synthesis of SiO₂ enriched in ¹⁷O. For the present synthesis, excess enriched water was used as the suspending liquid (rather than diethyl ether, used in the Si¹⁷O₂ synthesis).¹¹ This was done to preclude oxygen scrambling due to the relatively high solubility of GeO₂ in ether. The yield of 250 mg of Ge¹⁸O₂ from 3 g H₂¹⁸O was only 3% of the theoretical yield. No attempt was made to recover the excess H₂¹⁸O which was evaporated from the powder. The product was a finely divided off-white powder shown by Raman spectroscopy to be poorly crystallized hexagonal GeO₂. The -25-cm⁻¹ isotope shift of the main Raman line verified that the GeO₂ powder was ~98 at. % ¹⁸O enriched. This powder was melted into a glass sample by procedures to be described later in this section.

The ¹⁶O sample with natural-abundance Ge (and oxygen) was obtained as a high-purity (99.999%-pure) powder from Alfa Products.¹²

The ⁷⁰Ge and ⁷⁴Ge samples with natural-abundance O (atomic wt. ~16) were purchased as powdered GeO₂ from Oak Ridge National Laboratories.⁹ The raw materials were 98.6 at. % ⁷⁰Ge and 98.9 at. % ⁷⁴Ge, respectively. A significantly larger change in mass could have been achieved by using ⁷⁶Ge rather than ⁷⁴Ge but the ⁷⁶Ge stable isotope was prohibitively expensive.¹³

The powdered materials were fabricated into glass sam-

ples as follows. 200-mg charges of the ^{70}Ge (and ^{74}Ge) powders were melted in air at 1200°C for several hours in $11 \times 5 \times 4 \text{ mm}^3$ rectangular Pt boats. This resulted in clear vitreous samples containing a few fine bubbles. These samples were annealed at 1100°C for 1 h and air quenched. The Pt boats were cut and peeled from the samples leaving free-standing pieces of glass with smooth surfaces, which showed no strain under crossed polarizers. The samples were mounted in a holder which allowed the scattered light to be collected from the long face of the sample bottom, thus obviating polishing of the samples.

The ^{18}O -enriched GeO_2 powder was melted at 1200°C for several hours and annealed at 1100°C for 1 h in a Pt crucible. The melting and annealing were done in a sealed quartz tube to prevent oxygen exchange. The powder was first sintered in air for 20 min at 1200°C to produce a solid mass in the Pt crucible. This facilitated sealing the sample in a quartz tube and resulted in less than 3% oxygen exchange. (This estimate is based on a previous experiment in which a small amount of Ge^{18}O_2 powder was melted in air at 1200°C for 6.5 h; the Raman spectrum of this glass indicated that about 50% of the ^{18}O had been exchanged for ^{16}O .) We encountered some difficulty in peeling the Pt boat free of this sample; however, a shard of colorless virtually bubble-free $v\text{-GeO}_2$ enriched to $\sim 95\%$ ^{18}O was obtained.

We found the $v\text{-GeO}_2$ spectra to be rather insensitive to thermal history in the range employed. For example, there were no observable variations in peak wave number ($\pm 2 \text{ cm}^{-1}$) or relative line strength ($\pm 5\%$) for a sample which was water quenched after annealing at 800°C , or 900°C , or air quenched after annealing at 1100°C . Nevertheless, we made a point of annealing and quenching all samples in the same way.

EXPERIMENTAL RESULTS

The HH - and HV -polarized Raman spectra were obtained in the 90° scattering configuration using the 4579-\AA radiation from a Coherent Radiation Inc. CR12 Ar^+ -ion laser, a Spex 1401 double monochromator, and a RCA 31034A GaAs photomultiplier. The spectral slit width was less than 5 cm^{-1} throughout the spectral range utilized.

The resultant polarized spectra for $v\text{-Ge}^{16}\text{O}_2$ are shown in Fig. 1(a). These data show evidence for slight polarization scrambling, associated with the imperfect surfaces of the samples and the very small bubbles observed in the sample interior. Thus, the polarization ratio of the dominant line at 420 cm^{-1} is $I_{HH}/I_{HV} \approx 11$, substantially smaller than the value of 50 that has been reported¹⁴ in very pure bubble-free and well-annealed bulk samples of natural-abundance $v\text{-GeO}_2$. The effect of reduced polarization ratio is to produce no perceptible change in the HH spectrum, but to add relative strength to the 420-cm^{-1} line in the HV spectrum. We emphasize that the observed polarization scrambling is too small to influence the results used in this paper.

The broad features marked ω_i in Fig. 1(a) have been ascribed to the host disordered network of the glass,¹⁵ while the narrow features X_i are considered to be of unproven

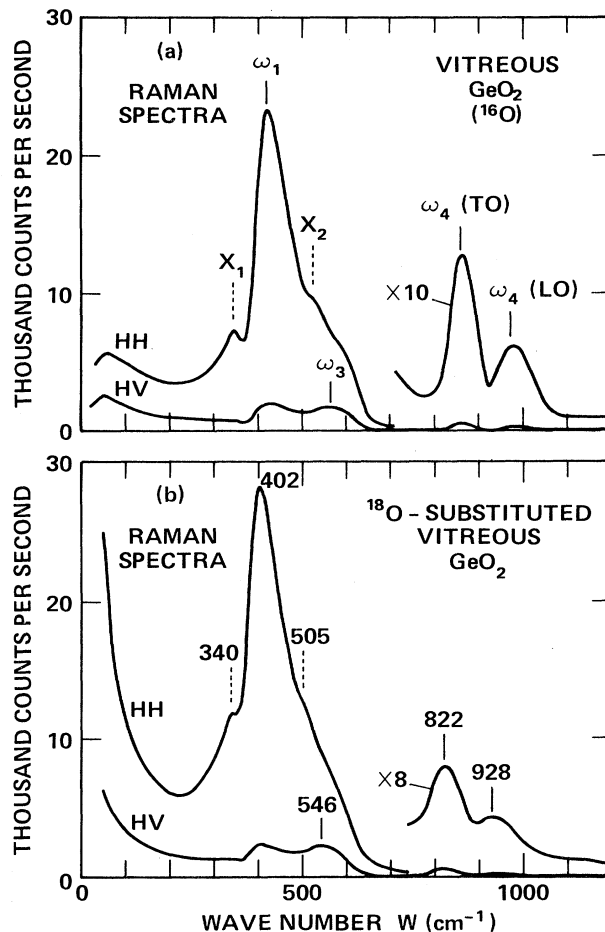


FIG. 1. Polarized Raman spectra of vitreous GeO_2 containing (a) 99.8 at. % ^{16}O and (b) 95 at. % ^{18}O . Network (ω_i), defect (X_2), and unknown origin (X_1) lines exhibit the $^{16}\text{O} \rightarrow ^{18}\text{O}$ isotope shifts listed in Table I.

origin. Because X_2 increases with neutron bombardment, it has been called a "defect" line.¹⁶ Since X_1 aligns with an infrared-determined longitudinal-optical (LO) frequency, this sharp feature has been termed an LO mode¹⁴; however, the LO assignment has been strongly questioned in recent work.^{17,18}

The polarized Raman spectra for $v\text{-Ge}^{18}\text{O}_2$ are shown in Fig. 1(b). They are qualitatively similar to the spectra for natural-abundance (^{16}O) material shown in Fig. 1(a).

We shall discuss the first order features with the aid of Table I, in which the lines are grouped according to their assumed physical origin: network, "defect," or unknown. The observed positions of all first-order Raman lines for $v\text{-Ge}^{18}\text{O}_2$ are listed in column (a), while those for $v\text{-Ge}^{16}\text{O}_2$ prepared under the same conditions are given in column (b). The observed shift Δ induced by substitution of ^{18}O for ^{16}O is given in column (c). The spectra were taken with expanded scales at least four times and the peak positions were determined by bisecting the features at several signal levels; this enabled us to project a position for the peak, whose uncertainty is measured by the numbers in parentheses in column (c). Note the larger uncer-

TABLE I. Comparison of the observed positions (cm^{-1}) of the first-order Raman spectral features in vitreous Ge^{18}O_2 with those of vitreous Ge^{16}O_2 . Observed isotope shifts Δ are compared with theoretical values Δ_{CF} calculated using the NN-CF-ICRN model developed in Refs. 15 and 19. Experimental uncertainties are given in parentheses in column (c). Comparison of columns (c) and (d) shows that the oxygen shifts of the high-frequency lines ω_3 and $\omega_4(\text{TO},\text{LO})$ are predicted quite well by the CF model, while the shift of the dominant Raman line ω_1 is too small for the CF theory. Other estimates correspond to assumptions of oxygen motion only (Δ_{O}), motion of an isolated Ge-O pair (Δ_{μ}), and germanium motion only (Δ_{Ge}). *Those estimates that are consistent with the observations, within the experimental error, are placed in square brackets, [].* Thus column (h) indicates that the ω_1 isotope shift is consistent with a significant admixture of Ge motion, like that in a Ge-O pair. The shift in X_1 suggests largely Ge motion, while that of X_2 is consistent with largely O motion, or with Ge-O motion.

Label	Origin of feature	Measured in spectrum	Observations			CF		Other estimates			
			(a) Ge^{18}O_2	(b) Ge^{16}O_2	(c) $\Delta=(a)-(b)$	(d) $\Delta_{\text{CF}}=(e)-(f)$	(e) Ge^{18}O_2	(f) Ge^{16}O_2	(g) Δ_{O}	(h) Δ_{μ}	(i) Δ_{Ge}
ω_1	Network	HH	402	420	$-18(\pm 2)$	-24	394	418	-24	[-20]	0
ω_3	Network	HH	546	563	$-17(\pm 2)$	[-17]	537	554	-32	-26	0
$\omega_4(\text{TO})$	Network	HH;HV	822	861	$-39(\pm 2)$	[-39]	(780)	(819)	-49	[-40]	0
$\omega_4(\text{LO})$	Network	HH;HV	928	973	$-45(\pm 2)$	[-45]	886	931	-56	[-45]	0
X_1	Unknown	HH	340	345	$-5(\pm 3)$				-20	-16	0
X_2	"Defect"	HH	505	530	$-25(\pm 7)$				[-30]	[-25]	0

tainty associated with the weak feature X_2 . Also note that the shifts are relatively large compared to their uncertainties (except for X_1 which shows a surprisingly small shift).

The shifts upon $^{70}\text{Ge} \rightarrow ^{74}\text{Ge}$ substitution were so small that the spectra were qualitatively indistinguishable from Fig. 1(a). The new spectra are therefore not shown. Instead, the observed positions are listed in columns (a) and (b) of Table II, and the resultant isotopic shifts in column (c). Note that the uncertainty in the shift of X_2 is not quite as large as before (because the overall spectral shape is unchanged). Otherwise, the uncertainties are essentially as before, and the germanium shifts are therefore determined with much less precision than the oxygen shifts.

COMPARISON WITH THEORIES

The observed isotopic shifts will be compared with various theoretical estimates which are presented in columns (d)–(i) of Tables I and II.

The theoretical shifts in column (d) are based on the

nearest-neighbor (NN) central-force (CF) idealized continuous–random-network (ICRN) model, first proposed by Sen and Thorpe¹⁹ and developed for application to Raman data by Galeener.¹⁵ According to this theory the (broad) network lines are given by

$$\omega_1^2 = (\alpha/M_{\text{O}})(1 + \cos\theta), \quad (1)$$

$$\omega_3^2 = (\alpha/M_{\text{O}})(1 + \cos\theta) + (4\alpha/3M_{\text{Ge}}), \quad (2)$$

$$\omega_4^2(\text{LO}) = (\alpha/M_{\text{O}})(1 - \cos\theta) + (4\alpha/3M_{\text{Ge}}), \quad (3)$$

where α is the CF constant, θ is the most probable value of the Ge-O-Ge angle, and M_{O} and M_{Ge} are the oxygen and germanium masses. This model was previously fit to data on natural-abundance $\nu\text{-GeO}_2$ in Ref. 15, with the result that $\theta = 128^\circ$ and $\alpha = 431 \text{ N/m}$. Using these values, $M_{\text{Ge}} = 72.6$ (for natural abundance) and $M_{\text{O}} = 18$, we predicted three of the frequencies in column (e) of Table I, while column (f) was obtained using $M_{\text{O}} = 16$. The fourth frequency ω_4 [transverse optical (TO)] is listed in

TABLE II. Comparison of the observed positions (cm^{-1}) of the first-order Raman spectral features in vitreous $^{74}\text{GeO}_2$ with those of vitreous $^{70}\text{GeO}_2$. Observed isotope shifts Δ are compared with theoretical values Δ_{CF} calculated using the NN-CF-ICRN model developed in Refs. 15 and 19. Experimental uncertainties are given in parentheses in column (c). Comparison of columns (c) and (d) shows that the germanium isotope shifts for ω_1 , ω_3 , and $\omega_4(\text{TO},\text{LO})$ are all consistent with the CF model within experimental uncertainty. Because the observed shifts Δ are small, ω_1 , X_1 , and X_2 are consistent with both oxygen motion only (Δ_{O}) and with motion of an isolated Ge-O pair (Δ_{μ}). No feature is consistent with germanium motion only (Δ_{Ge}). *Those estimates that are consistent with the observations, within experimental uncertainty, are placed in square brackets, [].* Ambiguities are partially resolved by comparison with the oxygen-shift data in Table I.

Label	Origin of feature	Measured in spectrum	Observations			CF theory		Other estimates			
			(a) $^{74}\text{GeO}_2$	(b) $^{70}\text{GeO}_2$	(c) $\Delta=(a)-(b)$	(d) $\Delta_{\text{CF}}=(e)-(f)$	(e) $^{74}\text{GeO}_2$	(f) $^{70}\text{GeO}_2$	(g) Δ_{O}	(h) Δ_{μ}	(i) Δ_{Ge}
ω_1	Network	HH	417	415	$-2(\pm 3)$	[0]	418	418	[0]	[-2]	-11
ω_3	Network	HH	560	565	$-5(\pm 2)$	[-7]	552	559	0	[-3]	-15
$\omega_4(\text{TO})$	Network	HH;HV	858	863	$-5(\pm 2)$	[-3]	(817)	(820)	0	[-4]	-24
$\omega_4(\text{LO})$	Network	HH;HV	970	970	$-6(\pm 2)$	[-4]	930	934	0	[-5]	-27
X_1	Unknown	HH	343	345	$-2(\pm 2)$				[0]	[-2]	-9
X_2	"Defect"	HH	530	530	$0(\pm 4)$				[0]	[-3]	-15

parentheses because it is given by the calculated $\omega_4(\text{LO})$ minus the *observed* TO-LO splitting [taken from columns (a) and (b)]. There is presently no way to make an *a priori* prediction of the TO-LO splitting in a glass.^{14,20,21} The differences between columns (e) and (f) are taken as the theoretically predicted isotope shifts entered in column (d).

The oxygen isotope shifts [column (c) of Table I] for the high frequency modes ω_3 , $\omega_4(\text{TO})$, and $\omega_4(\text{LO})$ are in excellent agreement with the predictions [column (d)]. These infrared-active lines¹⁴ correspond to the δ functions in the vibrational density of states of the Sen-Thorpe model,¹⁹ and the predictive value of the NN-CF-ICRN model is supported for these modes. *Here, and in the rest of the tables, those calculated shifts which are consistent with experiment within the estimated experimental error are enclosed in square brackets, []*.

The oxygen isotope shift of ω_1 is significantly less than predicted by the NN-CF-ICRN theory. As we shall show, this indicates the involvement of Ge motion, *none* of which is predicted by Eq. (1). We have previously reported evidence for Si motion in the ω_1 mode of ν -SiO₂ and ascribed it to an effect of real disorder in the glass that is not included in the ICRN structural model. A detailed description of that effect can be found in Ref. 2.

Since the X_1 and X_2 lines are not due to the ICRN, their shifts are not compared with any of Eqs. (1)–(3). We thus find it informative to compare our observations with expressions which describe simple limiting cases where the exact structure need not be specified.

The first of these is the assumption that a given mode frequency depends only on the oxygen mass, according to

$$\omega^2 = k/M_{\text{O}}, \quad (4)$$

where k is an effective force constant not dependent on M_{O} . This is therefore of the same form as Eq. (1) and predicts the same isotope shift, given by

$$\Delta_{\text{O}} \equiv \omega' - \omega = \omega[(M_{\text{O}}/M'_{\text{O}})^{1/2} - 1], \quad (5)$$

where the prime denotes the heavier mass. For $^{16}\text{O} \rightarrow ^{18}\text{O}$ the result is $\Delta_{\text{O}} = -0.0572\omega$. These shifts are given in column (g) of Table I using ω from column (b). The X_2 line is the only one whose shift is consistent with oxygen motion only. Note that the greatest percent discrepancy between columns (b) and (g) is for the X_1 line, which must therefore involve significant Ge motion.

A second simple model assumes Ge motion only with frequencies given by

$$\omega^2 = k/M_{\text{Ge}} \quad (6)$$

and resultant isotopic shifts given by

$$\Delta_{\text{Ge}} \equiv \omega' - \omega = \omega[(M_{\text{Ge}}/M'_{\text{Ge}})^{1/2} - 1]. \quad (7)$$

For oxygen substitution these shifts are all zero, as listed in column (i) of Table I. Thus, no experimental oxygen isotope shift is consistent with the assumption of Ge motion only.

Our third and last simple assumption is that the oxygen and germanium masses are both involved, as in a diatomic O-Ge “molecule” according to

$$\omega^2 = k/\mu, \quad (8)$$

where

$$\mu^{-1} = M_{\text{O}}^{-1} + M_{\text{Ge}}^{-1} \quad (9)$$

is the effective mass in the center-of-mass system of an O-Ge pair. The resultant isotopic shift is given by

$$\Delta_{\mu} \equiv \omega' - \omega = \omega[(\mu/\mu')^{1/2} - 1], \quad (10)$$

where the prime denotes the heavier effective mass. For $^{16}\text{O} \rightarrow ^{18}\text{O}$ the result is $\Delta_{\mu} = -0.0466\omega$, and this gives the predictions in column (h) using ω from column (b). Thus, the dominant Raman line ω_1 shifts by an amount consistent with Eq. (8), as do $\omega_4(\text{TO}, \text{LO})$ and X_2 . These correspondences do *not* tell us the exact amount of Ge involvement. In ω_1 or X_2 , for example, the extent could be as large as that in an isolated O-Ge pair. Note that X_1 seems to have much more Ge motion and is nearly consistent with Ge motion only.

We have also tested the possibility that the frequencies vary according to $\omega^2 = k/(M_{\text{O}} + M_{\text{Ge}})$, with negative result for all lines, under oxygen *and* germanium substitutions.

Comparisons of the aforementioned “theories” with the $^{70}\text{Ge} \rightarrow ^{74}\text{Ge}$ results are shown in Table II. The large number of entries in square brackets suggests that the data are consistent with several of the models; i.e., the small Ge shifts Δ are not determined precisely enough to differentiate completely among the models. For this reason we will take the correspondences in Table I more seriously. In any case, however, the Ge substitution data is clearly *inconsistent* with Ge only motion for any of the lines, and is also clearly *inconsistent* with oxygen only motion for ω_3 and $\omega_4(\text{TO}, \text{LO})$. These definite statements were also supported by the oxygen-substitution data of Table I.

DISCUSSION

We shall first draw some general conclusions by combining the correspondences indicated by square brackets in Tables I and II.

Network lines

The NN-CF-ICRN theory is adequate to predict the oxygen and germanium isotope shifts of the $\omega_3, \omega_4(\text{TO})$ and $\omega_4(\text{LO})$ network lines. This theory is *not* fully adequate for the dominant Raman line ω_1 since the experimental shifts indicate Ge motion not predicted by the theory. This cation motion is probably due to the disorder that exists in the glass but not in the theory, as discussed in Ref. 2 for ν -SiO₂. It is unlikely to be accounted for by mixing of the symmetric stretch motion¹⁵ with the rocking modes¹⁵ that are left out of the NN-CF-ICRN model; this mixing is much larger in ν -SiO₂ than in ν -GeO₂.²² The fact that the measured shifts in $\omega_4(\text{TO}, \text{LO})$ also agree with Δ_{μ} in Tables I and II is an accident associated with the near equality of $(1 - \cos\theta)$ and $\frac{4}{3}$ in Eq. (3).

These observations point to the need to compare results with a network theory which properly includes the noncentral forces. It will be interesting to see if inclusion of non-

central forces alone will describe the isotope shifts in ω_1 or if more realistic disorder is also required.

"Defect" line X_2

The isotopic shifts of the "defect" line X_2 are consistent with oxygen motion only, but they are also consistent with an admixture of Ge motion as large as that in an isolated Ge-O system. This uncertainty is due to the weakness of X_2 and the subsequent imprecision of its measured frequency. On the other hand, X_2 has been observed¹⁶ to increase with neutron bombardment like the ring defect line at 606 cm^{-1} in $\nu\text{-SiO}_2$, and the latter has oxygen motion only.^{1,2} We therefore tentatively assign X_2 to a regular ring of the type discussed in Ref. 6. The ring may be fourfold or threefold, but is almost certainly not twofold. This speculative assignment will be tested by comparison of the frequency of X_2 with that of the dominant Raman lines of threefold and fourfold cyclic germoxane molecules when measurements on the latter become available.²³

Line of unknown origin X_1

The oxygen isotope shift of X_1 is surprisingly small (-5 cm^{-1}) and quite inconsistent with oxygen motion only or even with isolated Ge-O motion. (See Table I.) We therefore suspect that X_1 cannot be associated with a regular ring, since in all other reported cases¹⁻⁶ the isotope shifts of the dominant Raman lines of regular rings show oxygen motion almost exclusively. In contrast, the isotopic shift data for X_1 are consistent with largely Ge motion, involving a modest admixture of O motion. That is, the shift lies somewhere between columns (h) and (i) in Tables I and II.

In the absence of an identification for X_1 , we offer the following comments. The X_1 line is sharp and highly polarized. This suggests a symmetric stretch motion,^{24,25} which with other observations¹⁷ argues against the original¹⁴ LO assignment. The very large component of Ge motion might suggest a Ge-Ge defect or a three-bonded Ge atom, but these structures seem to be ruled out by the failure of X_1 to increase in Ge-rich samples.¹⁶ It is certain that this region of the spectrum (below about 400 cm^{-1}) involves "rocking" and acoustic modes, as described in Ref. 18. Therefore, an explanation of X_1 may depend upon proper inclusion of noncentral forces in the vibrational theory. In that case X_1 may be due to the host network, but this seems inconsistent with the narrow width.

In preliminary work on isotopic shifts in $\nu\text{-As}_2\text{O}_3$ we observe a sharp low-frequency line which is due largely to As motion in puckered threefold rings,²⁶ but this motion is due to the three-connected nature of the As atoms and would not be expected for tetrahedrally connected Ge atoms (even in puckered rings). Until better arguments are found, we must consider X_1 to be of unknown origin, perhaps associated with noncentral forces in the host network.

GENERAL COMMENTS

A principal result of this study is to suggest the need for a dynamical analysis which includes noncentral forces and is capable of predicting small isotope shifts. An analytical theory like the Bethe-lattice²⁷ or a non-CF extension of the NN-CF-ICRN theory^{15,19} is likely to give the necessary precision, which is more difficult to obtain with a finite-cluster calculation like that of Bell and co-workers.²⁸

The existence of two unexplained features (X_1 and X_2) raises questions about the completeness of the CRN model. For example, small-order rings may have to be introduced (to account for X_2) or perhaps other perturbative departures from the CRN model will be required. Diffraction data supporting the basic CRN as a first-order model has been discussed by Leadbetter and Wright,²⁹ Sayers, Stern, and Lytle,³⁰ and more recently by Wright *et al.*³¹ Other Raman^{32,14} and infrared^{33,13} data, which have not focussed on X_1 and X_2 , have been said to support the CRN model,¹⁵ as have the large-cluster calculations of Bell and co-workers,²⁸ and the analysis of inelastic neutron scattering studies by Galeener, Leadbetter, and Stringfellow.¹⁸

More recently, Phillips³⁴ has suggested that X_1 and X_2 are evidence for a radically different structural model in which $\nu\text{-GeO}_2$ consists of microcrystalline clusters. He proposed that the two lines are due to dangling oxygen atoms on the cluster surfaces; however, this now seems unlikely because the isotopic shifts expected for such Ge-O systems are inconsistent with our observations of mostly oxygen motion (X_2) and mostly Ge motion (X_1).

ACKNOWLEDGMENTS

We are grateful to the U. S. Office of Naval Research (G. B. Wright) for support of this work under Contract No. N00014-80-C-0713.

*Present address: Clorox Technical Center, Pleasanton, CA 94566.

†Present address: Sandia Laboratories, Albuquerque, NM 87185.

¹F. L. Galeener and J. C. Mikkelsen, Jr., *Phys. Rev. B* **23**, 5527 (1981).

²F. L. Galeener and A. E. Geissberger, *Phys. Rev. B* **27**, 6199 (1983).

³F. L. Galeener and A. E. Geissberger, *J. Phys. (Paris) Colloq.* **44**, C9-343 (1983).

⁴C. F. Windisch and W. M. Risen, Jr., *J. Non-Cryst. Solids* **48**, 307 (1982).

⁵F. L. Galeener, *J. Non-Cryst. Solids* **49**, 53 (1982).

⁶F. L. Galeener, *Solid State Commun.* **44**, 1037 (1982).

⁷F. L. Galeener, in *The Structure of Non-Crystalline Materials II*, edited by P. H. Gaskell, A. E. Davis, and J. N. Parker (Taylor and Francis, London, 1983), p. 337.

⁸D. L. Griscom, in *Borate Glasses*, edited by L. D. Pye, V. D. Frechette, and N. J. Kreidl (Plenum, New York, 1978), p. 11.

⁹Isotope Sales, Oak Ridge National Laboratories, P.O. Box X,

- Oak Ridge, TN 37830.
- ¹⁰J. A. Abys, D. M. Barnes, S. Feller, G. Rouse, and W. M. Reisen, Jr., *Mater. Res. Bull.* **15**, 1581 (1980).
- ¹¹A. E. Geissberger and P. J. Bray, *J. Non-Cryst. Solids* **54**, 121 (1983).
- ¹²Alfa Products, Thiokol/Ventron Division, P.O. Box 299, 152 Andover St., Danvers, MA 01923.
- ¹³GeO₂ powder with 92.8 at. % ⁷⁶Ge is priced at \$8200 per gram when available from ORNL (Ref. 9).
- ¹⁴F. L. Galeener and G. Lucovsky, *Phys. Rev. Lett.* **37**, 1474 (1976).
- ¹⁵F. L. Galeener, *Phys. Rev. B* **19**, 4292 (1979).
- ¹⁶F. L. Galeener, *J. Non-Cryst. Solids* **40**, 527 (1980).
- ¹⁷See Sec. III E of Ref. 18.
- ¹⁸F. L. Galeener, A. J. Leadbetter, and M. W. Stringfellow, *Phys. Rev. B* **27**, 1052 (1983).
- ¹⁹P. N. Sen and M. F. Thorpe, *Phys. Rev. B* **15**, 4030 (1977).
- ²⁰F. L. Galeener, G. Lucovsky, and R. H. Geils, *Solid State Commun.* **25**, 405 (1978).
- ²¹R. M. Pick and M. Yvinec, in *Lattice Dynamics*, edited by M. Balkanski (Flammarion, Paris, 1978), p. 459.
- ²²E. Martinez (private communication). See also Ref. 2.
- ²³Such experiments are planned on cyclic germoxane molecules to be prepared by one of the authors (G.W.O).
- ²⁴F. L. Galeener, *J. Phys. (Paris) Colloq.* **42**, C6-24 (1981).
- ²⁵R. M. Martin and F. L. Galeener, *Phys. Rev. B* **23**, 3071 (1981).
- ²⁶F. L. Galeener and A. E. Geissberger (unpublished).
- ²⁷R. B. Laughlin, J. D. Joannopoulos, C. A. Murray, K. J. Hartnett, and T. J. Greytak, *Phys. Rev. Lett.* **40**, 461 (1978).
- ²⁸For a review of large-cluster calculations including non-central forces, see R. J. Bell, in *Methods in Computational Physics*, edited by G. Gilat (Academic, New York, 1976), p. 215.
- ²⁹A. J. Leadbetter and A. C. Wright, *J. Non-Cryst. Solids* **7**, 37 (1972).
- ³⁰D. E. Sayers, E. A. Stern, and F. W. Lytle, *Phys. Rev. Lett.* **35**, 584 (1975).
- ³¹A. C. Wright, G. Etherington, J. A. E. Desa, R. N. Sinclair, G. A. N. Connell and J. C. Mikkelsen, Jr., *J. Non-Cryst. Solids* **49**, 63 (1982).
- ³²S. K. Sharma, D. Virgo, and I. Kushiro, *J. Non-Cryst. Solids* **33**, 235 (1979).
- ³³B. T. K. Chen and G. J. Su, *Phys. Chem. Glasses* **12**, 33 (1971).
- ³⁴J. C. Phillips, *Solid State Phys.* **37**, 93 (1982).